Charge density wave fluctuation driven composite order in layered kagome metals

Alexei M. Tsvelik and Saheli Sarkar*

Division of Condensed Matter Physics and Materials Science, Brookhaven National Laboratory, Upton, New York 11973-5000, USA

(Received 6 April 2023; revised 21 June 2023; accepted 21 June 2023; published 12 July 2023)

The recently discovered kagome metals AV_3Sb_5 (A = K, Rb, Cs) offer an exciting route to study exotic phases arising due to interplay between electronic correlations and topology. In addition to superconductivity, these materials exhibit a charge-density-wave (CDW) phase occurring at ∼100 K, whose origin still remains elusive. The robust multicomponent 2×2 CDW phase in these systems is of great interest due to the presence of an unusually large anomalous Hall effect. In quasi-two-dimensional systems with weak interlayer coupling, fluctuation-driven exotic phases may appear. In systems with multicomponent order parameters, fluctuations may lead to establishment of composite order when only products of individual order parameters condense while the individual ones themselves remain disordered. We argue that such a fluctuation-driven regime of composite CDW order may exist in thin films of kagome metals above the CDW transition temperature. It is suggested that the melting of the trihexagonal state in the material doped away from the Van Hove singularities gives rise to a pseudogap regime where the spectral weight is concentrated in small pockets and most of the original Fermi surface is gapped. Our findings suggest the possible presence of exotic phases in the weakly coupled layered kagome metals, more so in the recently synthesized thin films of kagome metals.

DOI: 10.1103/PhysRevB.108.045119

I. INTRODUCTION

The interplay between electronic correlations and topology is a major field of study in the condensed matter systems [1,2]. The recently discovered kagome metals AV_3Sb_5 (A = K, Rb, Cs) are quasi-two-dimensional (2D) systems with hexagonal lattice symmetry [3]. The band structure of the kagome metals exhibits flat band, saddle-point Van Hove singularities (VHSs) and a pair of Dirac points. Owing to such an electronic structure, these systems have created a platform to study exotic phases which can occur due to the presence of both correlations and topology [4,5].

All AV_3Sb_5's undergo a charge-density-wave (CDW) transition [6–10] at around temperature $T_{CDW} \sim 100$ K. Along with the emergence of the CDW order, experiments and theoretical studies have found different unusual properties, such as bond density modulations [11], a chiral flux phase [12,13], and a giant anomalous Hall effect [14–16] with time-reversal symmetry breaking [17–20], which can be associated with loop currents [21–23].

At much lower temperatures these materials may exhibit superconductivity [4,24–26] with $T_c \sim 1$ K. The nature of the superconducting phase is still under debate. Some experiments found the gap to be nodeless [27], some to contain nodes [28]. Theoretical studies suggest an unconventional nature of the superconductivity [29–33]. There have also been proposals of more exotic superconductivity like pair-density wave [34,35], charge $4e$ and charge $6e$ superconducting states [35], and nematicity [36–38].

There have been many works [39–44] to gain insight into the nature of the CDW phase. So far, it is well established that the CDW order of the kagome metals is a multicomponent ($3Q$) one, although the real space structure of the CDW phase still remains elusive. Experiments [45,46] observe both star of david (SOD) and trihexagonal (TRH) patterns in the 2D plane of these systems. Moreover, the CDW order doubles the unit cell in the (a,b) plane and hence has a robust 2×2 feature as found in scanning tunneling microscopy (STM) [6], angle-resolved photoemission spectroscopy (ARPES) [47], and x-ray [48] experiments. However, some x-ray and STM experiments found a modulation in the crystallographic c direction for the kagome metals with alkali atoms Rb and Cs. The simultaneous ordering of the CDW phase with commensurate momenta $3Q$ are believed to be driven by nested Fermi surface instabilities [29,30,49,50], enhanced through the presence of VHSs due to logarithmically diverging density of states at the VHS points [51] in 2D. In this paper, we explore the situation [29] of a $\frac{5}{12}$ filled band when the chemical potential lies at the VHS.

According to the Mermin-Wagner theorem [52], fluctuations are enhanced in low dimensions. The presence of strong fluctuations is well established in such quasi-2D systems as cuprates, iron-based superconductors [53] where they are responsible for a pseudogap phase [54–56], anomalous phonon softening [57], and different emergent orders [58–60]. These prototype examples indicate that fluctuations may also play an important role in the layered quasi-2D kagome metal materials. However, as of now, although authors of several theoretical works have considered a mean-field scenario of the CDW order parameters, the effect of fluctuations in kagome CDW metals has not been discussed. Their effect will become even more important in the kagome metal monolayers [61] and thin films [62–64].

In this paper, we go beyond the mean-field theory of the multicomponent CDW order and consider the fluctuations

*ssarkar@bnl.gov

in these orders within a Ginzburg-Landau (GL) free energy model. As its microscopic justification, we consider an effective low-energy theory [49] described by the patch model considering only the V atoms of AV_3Sb_5, giving rise to VHSs at the three **M** points in the Brillouin zone. We consider 2D systems where topologically nontrivial configurations of the order parameter fields—vortices—can melt away the CDW order and restore the original lattice symmetry without destroying the quasiparticle gaps. We find an interval of temperatures above the CDW phase transition where only a composite order of the three CDWs can exist while the individual CDW order parameters remain fluctuating. The latter ones condense at low temperatures.

We organize the rest of the paper as follows. In Sec. II, we present our working microscopic model which includes the interactions in the system, giving rise to the electronic CDW instability. Then in Sec. III, we perform the mean-field analysis of the CDW orders. In Sec. IV, we consider fluctuations of the CDW order parameters and present a GL free energy by incorporating the vortex configurations by means of dual fields. In Sec. V, we consider a simplified case, where only two CDW orders develop. We discuss appearance of the composite order in this model. Then in Sec. VI, we discuss the effects of doping away from the VHSs. We argue that melting of the TRH phase in a doped system leads to emergence of a pseudogap regime resembling the one observed in the underdoped cuprates. Finally, we give a conclusion of our work in Sec. VII.

II. MODEL

The goal of this paper is to describe fluctuations in the CDW regime of kagome metals described by the patch model adopted by Park *et al.* [49]. A similar model leading to the same GL energy was used in Ref. [11]. Both models consider just one vanadium orbital per site of the kagome lattice. The CDW order is believed to be electronically driven. However, there are some experiments which point to the role of phonons [65].

The first-principles calculations [4,66,67] for the kagome metals AV_3Sb_5 show saddle points at the $\mathbf{M}_a$ points of the hexagonal Brillouin zone, giving rise to the logarithmically divergent density of states. Hence, we consider an effective low-energy model which consideres only patches of the Fermi surface around the $\mathbf{M}_a$ points in the Brillouin zone (Fig. 1) of kagome metals AV_3Sb_5 and interactions among the fermionic states between these saddle points, as was done in Ref. [49].

The noninteracting Hamiltonian is given by

$$H_0 = \sum_{a=1}^{3} \sum_{|k|<\Lambda} c^{\dagger}_{a\sigma}(k)[\epsilon_a(k) - \mu]c_{a\sigma}(k), \tag{1}$$

where the single-electron dispersion close to the saddle points $\mathbf{M}_a$ are given by

$$\begin{aligned} \epsilon_1 &= k_1(k_1 + k_2), \\ \epsilon_2 &= -k_1 k_2, \\ \epsilon_3 &= k_2(k_1 + k_2), \\ k_{1,2} &= k_x \pm \sqrt{3}k_y, \end{aligned} \tag{2}$$

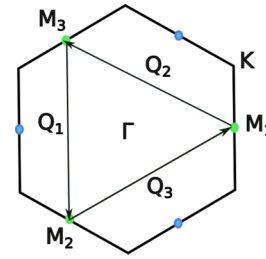

FIG. 1. The hexagonal Brillouin zone, showing the high-symmetry points. AV_3Sb_5 exhibits saddle points at $\mathbf{M}_{1,2,3}$, shown by green and blue circles. The $\mathbf{M}_a$ points are connected by the three nesting vectors $\mathbf{Q}_{1,2,3}$, which are also the ordering wave vectors of the charge density wave (CDW).

and μ is the chemical potential. Now we consider electron-electron interactions among the fermions in the three patches close to the M_a saddle points:

$$\begin{aligned} H_{\rm int} = \sum_{a\neq b} \sum_{k_1,k_2,k_3,k_4} \big[& g_1 \big(c^{\dagger}_{a,k_1,\sigma} c_{b,k_4,\sigma}\big)\big(c^{\dagger}_{b,k_2,\sigma'} c_{a,k_3,\sigma'}\big) \\ & + g_2 \big(c^{\dagger}_{a,k_1,\sigma} c_{a,k_4,\sigma}\big)\big(c^{\dagger}_{b,k_2,\sigma'} c_{b,k_3,\sigma'}\big) \\ & + g_3 \big(c^{\dagger}_{a,k_1,\sigma} c^{\dagger}_{a,k_2,-\sigma}\big)\big(c_{b,k_3,-\sigma} c_{b,k_4,\sigma}\big)\big] \\ & + \sum_{a} \sum_{k_1,k_2,k_3,k_4} g_4 \big(c^{\dagger}_{a,k_1,\sigma} c_{a,k_4,\sigma}\big)\big(c^{\dagger}_{a,k_2,-\sigma} c_{a,k_3,-\sigma}\big). \end{aligned} \tag{3}$$

The total effective Hamiltonian is given by

$$H = H_0 + H_{\rm int}. \tag{4}$$

In the Hamiltonian, $a = 1, 2, 3$ are the patch indices, and $\mathbf{k}$ is momentum measured from $\mathbf{M}_a$. In Eq. (3), we have the constraint $\mathbf{k}_1 + \mathbf{k}_2 + \mathbf{k}_3 + \mathbf{k}_4 = 0$. The coupling constants g_1, g_2, g_3, and g_4 represent interpatch exchange, interpatch density-density, Umklapp, and intrapatch scattering terms, respectively.

The parquet renormalization group (PRG) analysis [49] suggests that an instability in the system occurs if the corresponding interaction strength becomes positive. In this paper, we are interested only in various CDW instabilities. We do not consider [49] interplay between the superconductivity and the CDW, as the superconductivity appears only at very low temperature. Now one can construct the following CDW-type order parameters in the patch model.

For the real CDW (rCDW) and imaginary CDW (iCDW), the order parameters are, respectively,

$$\Omega_a \sim G_1 \sum_{k,\sigma} \big\langle c^{\dagger}_{a_2 k} c_{a_3 k'} \big\rangle, \tag{5}$$

$$\Psi_a \sim \frac{G_2}{i} \sum_{k,\sigma} \big\langle c^{\dagger}_{a_2 k} c_{a_3 k'} \big\rangle. \tag{6}$$

The effective interaction strengths for rCDW and iCDW are $G_1 = -2g_1 + g_2 - g_3$ and $G_2 = -2g_1 + g_2 + g_3$, respectively. Moreover, $\mathbf{k}' = \mathbf{k} + \mathbf{Q}_a$. Here, $\mathbf{Q}_a$'s are the three nesting vectors connecting $\mathbf{M}_a$ and the ordering wave vectors for the CDW order parameters, as shown in the Fig. 1.

The interactions are assumed to be quasilocal with Λ being the ultraviolet (UV) cutoff. The Hamiltonian is SU(2) $\times$ Z_3 $\times$ U(1) invariant.

III. MEAN-FIELD THEORY

In this section, we perform a mean-field decoupling of Eq. (4) in the CDW channels. This already suggests that we have $g_4 = 0$, as the effective interactions for rCDW and iCDW do not depend on g_4. We keep both rCDW and iCDW and derive a mean-field Hamiltonian and GL free energy in terms of complex CDW order parameters.

If the leading interaction term is g_1, one can perform the Hubbard-Stratonovich transformation:

$$H_{mf} = \frac{|V_{ab}|^2}{2g_1} + \sum_{a>b}[V_{ab}c^+_{a\sigma}c_{b\sigma} + V^*_{ab}c^+_{b\sigma}c_{a\sigma}] + \sum_{a=1}^{3}\sum_{|k|<\Lambda}\epsilon_a(k)c^+_{a\sigma}(k)c_{a\sigma}(k). \tag{7}$$

We introduce notations $V_{12} = \Delta_3$, $V_{13} = \Delta_2$, and $V_{23} = \Delta_1^*$. Now by integrating out the fermion field, we obtain the action in terms of the CDW order parameter fields $\Delta_a = \Omega_a + i\Psi_a = |\Delta_a|\exp(i\phi_a)$:

$$F = \frac{1}{2g_1}\int d^2x d\tau |\Delta_a|^2 - \mathrm{Tr}\ln\mathcal{G}^{-1}, \tag{8}$$

where $\mathcal{G}^{-1}$ is the inverse Green's function matrix. The electronic spectrum at the saddle point is determined by the equation:

$$\begin{vmatrix} -E+\epsilon_1 & \Delta_3 & \Delta_2 \\ \Delta_3^* & -E+\epsilon_2 & \Delta_1^* \\ \Delta_2^* & \Delta_1 & -E+\epsilon_3 \end{vmatrix} = 0. \tag{9}$$

The result is

$$(\epsilon_1 - E)(\epsilon_2 - E)(\epsilon_3 - E) + E(|\Delta_1|^2 + |\Delta_2|^2 + |\Delta_3|^2) - \epsilon_1|\Delta_1|^2 - \epsilon_2|\Delta_2|^2 - \epsilon_3|\Delta_3|^2 + \Delta_1\Delta_3\Delta_2 + \Delta_1^*\Delta_2^*\Delta_3^* = 0. \tag{10}$$

We assume that the fluctuations of moduli are gapped and consider the saddle point where all $|\Delta_a|$'s are equal. It follows from Eq. (2) that

$$\epsilon_1\epsilon_2 + \epsilon_1\epsilon_3 + \epsilon_2\epsilon_3 = 0, \tag{11}$$

which leads to simplification of Eq. (10), resulting in

$$(E \pm 1)^2(E \mp 2) - 3\left(k_x^2 + k_y^2\right)(E^2 - 1) + 4k_x^2\left(k_x^2 - 3k_y^2\right)^2 = 0, \tag{12}$$

where we set $|\Delta_a| = 1$. According to Ref. [33], a plus sign in the first bracket corresponds to the $-3Q$ phase (SOD). In this phase, there is a Fermi surface (see Fig. 2). The minus sign corresponds to the $+3Q$ (TRH) phase where the quasiparticle spectrum is fully gapped. At $g_3 \neq 0$, the mean-field spectrum should be corrected:

$$\Delta_a \to \Delta_a + \left(\frac{g_3}{g_1}\right)\Delta_a^*. \tag{13}$$

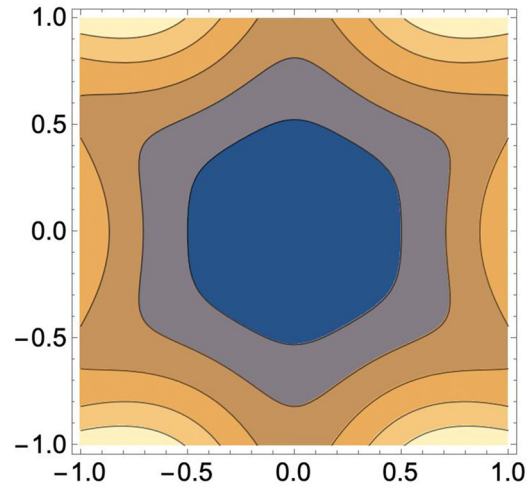

FIG. 2. Contour plots of the gapless quasiparticle branch in the $-3Q$ phase. The Fermi surface is the boundary between the gray and brown areas.

This change does not modify the spectrum qualitatively, though it modifies Green's function.

IV. GL FREE ENERGY

We will follow the conclusions of the previous papers and, as we have mentioned above, consider the saddle-point solution with all $|\Delta_a|$'s being equal and treat fluctuations of the moduli of Δ's as gapped. Hence, the subsequent analysis of the GL free energy will include only phase fluctuations. In the absence of the Umklapp $g_3 = 0$, the only phase-dependent term in the free energy density corresponds to the product of all three Δ's:

$$\delta F = -G\cos(\phi_1 + \phi_2 + \phi_3). \tag{14}$$

Hence, in the absence of the Umklapp, two phase fields remain critical in the low-temperature phase. However, if $g_3 \neq 0$, there is a contribution to the free energy density:

$$g_3\left[\Delta_a^2 + (\Delta_a^*)^2\right] \sim g_3[\cos(2\phi_1) + \cos(2\phi_2) + \cos(2\phi_3)]. \tag{15}$$

A. Fluctuations in the CDW order parameters

Now we will consider phase fluctuations of the CDW order parameters which requires inclusion of the gradient terms. In 2D, one must account for topologically nontrivial configurations of order parameter fields—vortices—which are pointlike objects with finite energy and can be thermally excited. To properly account for such configurations, we regularize the model by putting it on a suitable lattice with lattice constant b and then taking a continuum limit.

The form of the free energy functional in Eq. (16) reflects the fact that the order parameters are periodic functions of ϕ_a. This feature allows for topologically nontrivial configurations of the fields in the form of vortices—configurations where ϕ_a fields change by 2π along closed spacial loops. In the continuum limit, such configurations are singular, which explains the necessity for lattice regularization. It is well known that

in 2D vortices can change the character of phase transitions. One way to consider them in the continuous limit is to introduce dual phase fields $\bar{\phi}_a$ [68]. In the present case, this is slightly unusual because, in the region of interest, the GL action contains the terms which depend on both ϕ and $\bar{\phi}$. The corresponding formalism was introduced in Ref. [69] (see also Ref. [59]). The regularized GL free energy density is

$$\frac{\mathcal{F}}{T} = -\frac{J}{T}\sum_a \sum_{\langle b\rangle} \frac{1}{b^2}\cos\left[\phi_a(\mathbf{x}) - \phi_a(\mathbf{x}+\mathbf{b})\right] - G\cos(\phi_1+\phi_2+\phi_3) + Ag_3\sum_a \cos(2\phi_a), \quad (16)$$

where coefficient $A \sim \Delta^2/T > 0$.

Now we can follow the standard procedure and write the continuum limit of Eq. (16) as (in what follows, we will set the stiffness $J = 1$)

$$\frac{\mathcal{F}}{T} = \sum_a \left[\frac{1}{2T}(\partial_x\phi_a)^2 + \frac{T}{2}(\partial_x\bar{\phi}_a)^2 + i\partial_x\phi_a\partial_y\bar{\phi}_a + Ag_3\cos(2\phi_a) + \eta\cos(2\pi\bar{\phi}_a)\right] - G\cos(\phi_1+\phi_2+\phi_3). \quad (17)$$

The coupling η is proportional to the vortex fugacity. The model Eq. (17) contains both original fields ϕ_a and their dual fields $\bar{\phi}_a$ which take care of the vortex configurations. The corresponding path integral for the partition function includes integration over both fields:

$$Z = \int D\phi_a(x) D\bar{\phi}_a(x) \exp\left(-\int d^2x \frac{\mathcal{F}}{T}\right). \quad (18)$$

To determine whether the cosine terms are relevant or irrelevant, one has to calculate their scaling dimensions. To compute the scaling dimensions of various perturbations, we start with the Gaussian model. The results are

$$d_{g_3} = \frac{T}{\pi}, \quad d_\eta = \frac{\pi}{T}, \quad d_G = \frac{3T}{4}\pi. \quad (19)$$

The direct and dual operators cannot order simultaneously; this creates an interesting situation at the transition where both of them are relevant. It is a nontrivial situation, see for example, Ref. [59].

In what follows, we consider a limit of large G when the sum of all phases is fixed [31]. Now we can make a transformation as follows:

$$\phi_a = \frac{\Phi}{\sqrt{3}} + \left(\sqrt{\frac{2}{3}}\right)\mathbf{e}_a\boldsymbol{\chi}, \quad \mathbf{e}_a = (1,0), \quad \left(-\frac{1}{2}, \frac{\sqrt{3}}{2}\right), \quad \left(-\frac{1}{2}, -\frac{\sqrt{3}}{2}\right), \quad (20)$$

with $\boldsymbol{\chi} = (\chi_1, \chi_2)$ and treat Φ as gapped.

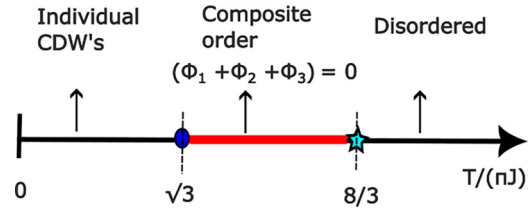

FIG. 3. The phase diagram of the kagome metal layer. For $J = 1$, there is a crossover into a regime with composite order around $\frac{T}{\pi} = \frac{8}{3}$, where the sum of the charge-density-wave (CDW) phases are frozen. For a doping slightly away from the Van Hove singularity (VHS; $\mu \neq 0$), it will exhibit a pseudogap-like behavior. Around $\frac{T}{\pi} = \sqrt{3}$, there is a phase transition into the state where individual CDWs order. For $g_3 > 0$, the low-temperature phase breaks time-reversal symmetry.

In this case, we get following the calculation shown in Appendix, an effective free energy:

$$\frac{\mathcal{F}_{\text{eff}}}{T} = \sum_{a=1}^{3}\left[\bar{A}g_3\cos\left(\sqrt{\frac{8}{3}}\mathbf{e}_a\boldsymbol{\chi}\right) - B\cos(2\pi\sqrt{2}\boldsymbol{\omega}_a\bar{\boldsymbol{\chi}})\right] + \sum_{i=1,2}\left[\frac{1}{2T}(\partial_x\chi_i)^2 + \frac{T}{2}(\partial_x\bar{\chi}_i)^2 + i\partial_x\chi_i\partial_y\bar{\chi}_i\right], \quad (21)$$

where $\boldsymbol{\omega}_a = (0,1), (\sqrt{3},1)/2, (\sqrt{3},-1)/2$, $B \sim \eta^2$, and $\bar{A} = \langle\cos(\Phi/\sqrt{3})\rangle A$.

The scaling dimensions of the cosines are

$$d_{g_3} = \frac{2T}{3\pi}, \quad d_B = \frac{2\pi}{T}. \quad (22)$$

The perturbations are relevant or irrelevant when the scaling dimension of the operators $d_{\text{op}} < D$ and $d_{\text{op}} > D$, respectively, D being the spatial dimension of the system. We observe that, below $T/\pi = 3$, both direct and dual cosine terms are relevant, provided the G term is relevant, which is true for $T/\pi < \frac{8}{3}$.

Below $T_{c1}/\pi = \frac{8}{3}$, the G term is relevant, and the sum of all phases is frozen. However, above a certain temperature T_{c2}, the vortices destroy the order of individual CDWs. Only the product of their order parameters acquires a finite average, which we refer to as a composite order $(\Delta_1\Delta_2\Delta_3)$ (see Fig. 3). Since the periodicity of this order parameter coincides with the periodicity of the lattice, T_{c1} is likely to mark a crossover.

At T_{c2}, there is a transition where individual phases are frozen which breaks the symmetry of the lattice and may also break the time-reversal symmetry (see below and see also Fig. 3). The character of the low-temperature phase is determined by the signs of G and g_3. At $G > 0$, the product of Δ's has the same sign, and we have the TRH order; at $G < 0$, it is negative, and we have the SOD pattern. If $g_3 < 0$, the vacuum corresponds to $\chi_1 = \chi_2 = 0$. This is rCDW. If $g_3 > 0$, there are degenerate vacua situated on a hexagonal lattice of $\chi_{1,2}$. There are two inequivalent points $\sqrt{\frac{8}{3}}(\chi_1, \chi_2) = (4\pi/3, 0)$ and $(2\pi/3, 2\pi/\sqrt{3})$. At each of these vacua, all Δ_a's are the same and are equal either to $\exp(4\pi i/3)$ or its complex conjugate. In the broken-symmetry state, one of this vacua is

chosen which corresponds to complex rCDW + iCDW with a broken time reversal. This time-reversal symmetry breaking spontaneously induces orbital currents which can manifest into the anomalous Hall effect [14]. The resulting real-space pattern for the corresponding bond order can be either SOD or TRH along with the current order pattern, as also discussed in Refs. [11,49].

The transition temperature is determined by the competition between normal and dual cosine perturbations. It can be estimated by comparing the mass scales generated by the competing operators. A relevant perturbation can drive a phase transition, and the transition point can be determined by estimating the scale of mass gaps in the corresponding phases and comparing them with each other. The scale of the mass gap can be estimated by the fact that the contribution to the action of the relevant operator inducing a finite correlation length becomes of the order of unity. Therefore, we notice that the phase transition from the composite order state to the state with individual CDWs occurs when

$$B^{1/(2-d_B)} \sim (\bar{A}g_3)^{1/(2-d_{g_3})}. \tag{23}$$

Solving this equation with logarithmic accuracy, we get the estimate for the transition temperature:

$$\frac{T_{c2}}{\pi} = \frac{3}{2}\left(1-\alpha+\sqrt{1-\frac{2\alpha}{3}+\alpha^2}\right),$$
$$\alpha = \frac{\ln(\bar{A}g_3)}{\ln B}. \tag{24}$$

For comparable coupling constants, it yields $T_{c2}/\pi = \sqrt{3}$ and $d^* = 2/\sqrt{3}$.

The model in Eq. (21) belongs to the class of affine XY models which have been studied in connection to the problem of quark confinement [70,71]. Although this model has not been studied, some insights can be drawn. An affine XY model with different operators was studied numerically in Ref. [71], and the results indicate that the transition is probably weak first order. The hysteresis, however, has not been observed, which leaves the possibility of a second-order phase transition. The uncertainty remains, and a first-order transition also remains a possibility for our case. If, however, it is a second-order transition, then following the results for another similar model [72], we suggest that it would belong to the $\mathbb{Z}_3$ Potts universality class [73]. This suggests that the critical exponents are $\nu = \frac{5}{6}$ and $\eta = \frac{4}{15}$ [74].

V. SIMPLIFIED CASE

The purpose of this section is to study an example of a treatable model describing a phase transition driven by mutually dual cosines. This model describes the case when only two CDWs develop: $\Delta_3 = 0$ and $|\Delta_1| = |\Delta_2|$, describing a nematicity [38] in the system. Then there are two phases ϕ_1 and ϕ_2, whose fluctuations are described by the action in Eq. (16). Once their sum is frozen, we arrive at the model [Eq. (21)] with a single pair of fields χ, $\bar{\chi}$. This situation was studied in Ref. [59], and we repeat the calculations here for illustrative purposes.

In this case, at $T/\pi = 1$, the scaling dimensions of the cosines are equal to 1, giving rise to comparable values of $\bar{A}g_3$ and B. At this point, the bosonic action [Eq. (21)] can be refermionized and recast as a model of relativistic fermions with two kinds of mass terms [75]:

$$\frac{\mathcal{F}_{\text{eff}}}{T} = R^+(\partial_y - i\partial_x)R + L^+(\partial_y + i\partial_x)L$$
$$+\bar{A}g_3(R^+L + L^+R) + B(RL + L^+R^+). \tag{25}$$

The next step is to express the Dirac fermions in terms of Majoranas:

$$R, L = \frac{1}{\sqrt{2}}[\rho^{(+)}_{R,L} + i\rho^{(-)}_{R,L}]. \tag{26}$$

As a result, we get two separate models for Majorana fermions with masses $m_\pm = \bar{A}g_3 \pm B$. Each Majorana species corresponds to the 2D Ising model where the mass is proportional to $(T - T_c)$. For any sign of g_3, the transition occurs only for one Majorana species. As was shown in Ref. [59], the CDW order parameter (for instance, Δ_1 since, in the given case, $\Delta_2 = \Delta_1^*$) can be written as

$$\Delta = i\sigma_+\sigma_- + \mu_+\mu_-, \tag{27}$$

where $\sigma_\pm$ are the order and $\mu_\pm$ are the disorder parameters of the Ising models with masses $m_\pm$. One of these models is always in the ordered $\langle\sigma\rangle \neq 0$ or disordered ($\langle\mu\rangle \neq 0$) phase; the other one undergoes a phase transition. It can be shown that, in the part of the phase diagram where $m_\pm > 0$, the expectation value of $\sigma_{1/2}$ is nonvanishing, whereas the average of $\mu_{1/2}$ vanishes. Also, for $m_\pm < 0$, the average of $\sigma_\pm$ vanishes, while the average of $\mu_\pm$ becomes finite.

The $\mathbb{Z}_3$ symmetric case is more complicated. If the transition is of the second order, then some insight can be drawn from Ref. [72], where a similar model at the transition point was represented as a sum of the critical $\mathbb{Z}_3$ Potts model and a W_3 conformal field theory perturbed by a relevant operator:

$$H = H^0_{\mathbb{Z}_3} + H^0_{W_3} - \gamma\Phi_{\lambda_1+\lambda_2,0}, \tag{28}$$

where λ's are fundamental weights of the SU(3) group. The perturbed W_3 theory is massive.

VI. DOPING

All previous calculations remain valid if the chemical potential is slightly away from the VHS. In the low-temperature state, the CDW order will lead to reconstruction of the Fermi surface through Brillouin zone folding with the appearance of small Fermi pockets, as described, for example, in Ref. [35]. Once the temperature exceeds T_{c2}, the individual CDW order will melt, but the spectral gaps will survive. The system will enter into a pseudogap regime like the one observed in the underdoped cuprates where, below a certain crossover temperature, most of the original Fermi surface gradually fades away, and the low-energy spectral weight is concentrated at small pockets. As in the cuprates, the predicted crossover is not accompanied by broken-lattice symmetry. The idea is that melting of the low-temperature Néel order may explain the observations of the Fermi surface arcs [76].

VII. CONCLUSIONS

In this paper, we have studied a fluctuation regime in the CDW order, within an effective low-energy interacting patch model [49] describing a layered kagome system or a 2D film. We study the fluctuation by considering a field theoretic technique which allows us to simultaneously treat the effects of the discrete symmetry-breaking order and the vortex physics. We observe that the interplay of fluctuations and topology (vortices) in 2D leads to formation of a special regime where the individual low-temperature CDW orders melt, restoring the lattice symmetry but keeping the quasiparticle gaps intact. At further lowering of the temperature, the system undergoes a transition into the phase with individual CDW order.

The suggested mechanism is like the mechanism of formation of charge $6e$ superconducting condensate described theoretically in Refs. [35,77–80] and recently observed in the thin flakes of the kagome superconductor CsV_3Sb_5 [81]. The measurements were performed on mesoscopic CsV_3Sb_5 rings fabricated by etching the kagome superconductor thin flakes exfoliated from bulk samples. We suggest a similar arrangement for the CDW experiments. We identify the CDW transition as belonging to the $\mathbb{Z}_3$ Potts universality class.

ACKNOWLEDGMENTS

We are grateful to Andrey Chubukov, Philippe Lecheminant, and Dmitry Kovrizhin for valuable discussions. We are grateful to Philippe Lecheminant for attracting our attention to several papers relevant to the present topic. This paper was supported by Office of Basic Energy Sciences, Material Sciences and Engineering Division, U.S. Department of Energy under Contract No. DE-SC0012704.

APPENDIX: FREE ENERGY FOR A LARGE VALUE OF G

The free energy considered in Sec. IV A is given by

$$\frac{\mathcal{F}}{T}=\sum_a\left[\frac{1}{2T}(\partial_x\phi_a)^2+\frac{T}{2}(\partial_x\bar\phi_a)^2+i\partial_x\phi_a\partial_y\bar\phi_a +Ag_3\cos(2\phi_a)+\eta\cos(2\pi\bar\phi_a)\right] -G\cos(\phi_1+\phi_2+\phi_3). \tag{A1}$$

At $\eta=0$, one can integrate over $\partial_x\bar\phi_a$:

$$\int D\bar\phi_a\exp\left\{-\int d^2x\left[\frac{T}{2}(\partial_x\bar\phi_a)^2+i\partial_x\phi_a\partial_y\bar\phi_a\right]\right\} =\text{const}\int D\bar\phi_a\exp\left\{-\int d^2x\left[\frac{T}{2}(\partial_x\bar\phi_a)^2-i\partial_y\phi_a\partial_x\bar\phi_a\right]\right\} \sim\exp\left[-\frac{1}{2T}\int d^2x(\partial_y\phi)^2\right]. \tag{A2}$$

The result is the partition function for ϕ fields:

$$Z[\phi]=\int D\phi_a\exp\left\{-\int d^2x\left[\frac{1}{2T}(\partial_x\phi_a)^2+(\partial_y\phi_a)^2\right] +Ag_3\cos(2\phi_a)-G\cos(\phi_1+\phi_2+\phi_3)\right\}. \tag{A3}$$

In a similar way, at $g_3=0$, we can integrate out the ϕ fields.

In the limit of large G, we can consider the sum of all phases to be fixed. Hence, the GL free energy can be transformed with

$$\phi_1=\frac{\Phi}{\sqrt3}+\left(\sqrt{\frac23}\right)\chi_1,\quad \phi_2=\frac{\Phi}{\sqrt3}+\left(\sqrt{\frac23}\right)\left(-\frac{\chi_1}{2}+\frac{\sqrt3}{2\chi_2}\right),\quad \phi_3=\frac{\Phi}{\sqrt3}-\left(\sqrt{\frac23}\right)\left(\frac{\chi_1}{2}+\frac{\sqrt3}{2\chi_2}\right). \tag{A4}$$

In this case, $\cos(\phi_1+\phi_2+\phi_3)=\cos(\sqrt3\Phi)$. When Φ is frozen, the dual field $\bar\Phi=\sum_a\bar\phi_a$ fluctuates strongly so that correlators of the dual exponents decay exponentially. Then the dual perturbation is generated in the second order in η:

$$\eta^2\int d^2x\exp\left\{\frac{i\bar\Phi}{\sqrt3}+\sqrt{\frac{8}{3\pi}}\mathbf{e}_a\bar{\boldsymbol\chi}\right\}_{\mathbf{r}} \times\exp\left\{-\frac{i\bar\Phi}{\sqrt3}-\sqrt{\frac{8}{3\pi}}\mathbf{e}_b\bar{\boldsymbol\chi}\right\}_{\mathbf{r}+\mathbf{x}}, \tag{A5}$$

giving rise to the operators

$$\cos\left[\sqrt{\frac83}\pi(\mathbf{e}_a-\mathbf{e}_b)\bar{\boldsymbol\chi}\right], \tag{A6}$$

with scaling dimension $2\pi/T$. In that case, we get

$$\frac{\mathcal{F}_{\text{eff}}}{T}=\sum_{a=1}^{3}\left[\bar Ag_3\cos\left(\sqrt{\frac83}\mathbf{e}_a\boldsymbol\chi\right)-B\cos(2\pi\sqrt2\boldsymbol\omega_a\bar{\boldsymbol\chi})\right] +\sum_{i=1,2}\left[\frac{1}{2T}(\partial_x\chi_i)^2+\frac{T}{2}(\partial_x\bar\chi_i)^2+i\partial_x\chi_i\partial_y\bar\chi_i\right], \tag{A7}$$

with $\boldsymbol\omega_a=(0,1),(\sqrt3,1)/2$, and $(\sqrt3,-1)/2$. More explicitly,

$$\sum_a\cos\left(\sqrt{\frac83}\mathbf{e}_a\boldsymbol\chi\right) =\cos\left[\sqrt{\frac83}\chi_1\right]+\cos\left[\sqrt{\frac23}(\chi_1-\sqrt3\chi_2)\right] +\cos\left[\sqrt{\frac23}(\chi_1+\sqrt3\chi_2)\right], \tag{A8}$$

and

$$\sum_a\cos(2\pi\sqrt2\boldsymbol\omega_a\bar{\boldsymbol\chi}) =\cos[2\pi\sqrt2\bar\chi_2]+\cos[\pi\sqrt2(\bar\chi_2+\sqrt3\bar\chi_1)] +\cos[\pi\sqrt2(\bar\chi_2-\sqrt3\bar\chi_1)]. \tag{A9}$$

[1] D. M. Kennes, M. Claassen, L. Xian, A. Georges, A. J. Millis, J. Hone, C. R. Dean, D. Basov, A. N. Pasupathy, and A. Rubio, Nat. Phys. **17**, 155 (2021).

[2] M. Dzero, J. Xia, V. Galitski, and P. Coleman, Annu. Rev. Condens. Matter Phys. **7**, 249 (2016).

[3] B. R. Ortiz, L. C. Gomes, J. R. Morey, M. Winiarski, M. Bordelon, J. S. Mangum, I. W. H. Oswald, J. A. Rodriguez-Rivera, J. R. Neilson, S. D. Wilson *et al.*, Phys. Rev. Mater. **3**, 094407 (2019).

[4] B. R. Ortiz, S. M. L. Teicher, Y. Hu, J. L. Zuo, P. M. Sarte, E. C. Schueller, A. M. M. Abeykoon, M. J. Krogstad, S. Rosenkranz, R. Osborn *et al.*, Phys. Rev. Lett. **125**, 247002 (2020).

[5] B. R. Ortiz, P. M. Sarte, E. M. Kenney, M. J. Graf, S. M. L. Teicher, R. Seshadri, and S. D. Wilson, Phys. Rev. Mater. **5**, 034801 (2021).

[6] Y.-X. Jiang, J.-X. Yin, M. M. Denner, N. Shumiya, B. R. Ortiz, G. Xu, Z. Guguchia, J. He, M. S. Hossain, X. Liu *et al.*, Nat. Mater. **20**, 1353 (2021).

[7] H. Li, T. T. Zhang, T. Yilmaz, Y. Y. Pai, C. E. Marvinney, A. Said, Q. W. Yin, C. S. Gong, Z. J. Tu, E. Vescovo *et al.*, Phys. Rev. X **11**, 031050 (2021).

[8] E. Uykur, B. R. Ortiz, S. D. Wilson, M. Dressel, and A. A. Tsirlin, npj Quantum Mater. **7**, 16 (2022).

[9] B. R. Ortiz, S. M. L. Teicher, L. Kautzsch, P. M. Sarte, N. Ratcliff, J. Harter, J. P. C. Ruff, R. Seshadri, and S. D. Wilson, Phys. Rev. X **11**, 041030 (2021).

[10] H. Tan, Y. Liu, Z. Wang, and B. Yan, Phys. Rev. Lett. **127**, 046401 (2021).

[11] M. M. Denner, R. Thomale, and T. Neupert, Phys. Rev. Lett. **127**, 217601 (2021).

[12] X. Feng, K. Jiang, Z. Wang, and J. Hu, Sci. Bull. **66**, 1384 (2021).

[13] L. Yu, C. Wang, Y. Zhang, M. Sander, S. Ni, Z. Lu, S. Ma, Z. Wang, Z. Zhao, H. Chen *et al.*, arXiv:2107.10714 (2021).

[14] S.-Y. Yang, Y. Wang, B. R. Ortiz, D. Liu, J. Gayles, E. Derunova, R. Gonzalez-Hernandez, L. Šmejkal, Y. Chen, S. S. Parkin *et al.*, Sci. Adv. **6**, eabb6003 (2020).

[15] F. H. Yu, T. Wu, Z. Y. Wang, B. Lei, W. Z. Zhuo, J. J. Ying, and X. H. Chen, Phys. Rev. B **104**, L041103 (2021).

[16] E. M. Kenney, B. R. Ortiz, C. Wang, S. D. Wilson, and M. J. Graf, J. Phys.: Condens. Matter **33**, 235801 (2021).

[17] C. Mielke, III, D. Das, J.-X. Yin, H. Liu, R. Gupta, Y.-X. Jiang, M. Medarde, X. Wu, H. Lei, J. Chang *et al.*, Nature (London) **602**, 245 (2022).

[18] R. Khasanov, D. Das, R. Gupta, C. Mielke, M. Elender, Q. Yin, Z. Tu, C. Gong, H. Lei, E. T. Ritz *et al.*, Phys. Rev. Res. **4**, 023244 (2022).

[19] R. Gupta, D. Das, C. Mielke, III, E. Ritz, F. Hotz, Q. Yin, Z. Tu, C. Gong, H. Lei, T. Birol *et al.*, arXiv:2203.05055 (2022).

[20] Y. Xu, Z. Ni, Y. Liu, B. R. Ortiz, Q. Deng, S. D. Wilson, B. Yan, L. Balents, and L. Wu, Nat. Phys. **18**, 1470 (2022).

[21] Y.-P. Lin and R. M. Nandkishore, Phys. Rev. B **104**, 045122 (2021).

[22] M. H. Christensen, T. Birol, B. M. Andersen, and R. M. Fernandes, Phys. Rev. B **106**, 144504 (2022).

[23] Y. Wang, S. Yang, P. K. Sivakumar, B. R. Ortiz, S. M. Teicher, H. Wu, A. K. Srivastava, C. Garg, D. Liu, S. S. Parkin *et al.*, arXiv:2012.05898 (2020).

[24] K. Y. Chen, N. N. Wang, Q. W. Yin, Y. H. Gu, K. Jiang, Z. J. Tu, C. S. Gong, Y. Uwatoko, J. P. Sun, H. C. Lei *et al.*, Phys. Rev. Lett. **126**, 247001 (2021).

[25] S. Ni, S. Ma, Y. Zhang, J. Yuan, H. Yang, Z. Lu, N. Wang, J. Sun, Z. Zhao, D. Li *et al.*, Chin. Phys. Lett. **38**, 057403 (2021).

[26] C. Mu, Q. Yin, Z. Tu, C. Gong, H. Lei, Z. Li, and J. Luo, Chin. Phys. Lett. **38**, 077402 (2021).

[27] W. Duan, Z. Nie, S. Luo, F. Yu, B. R. Ortiz, L. Yin, H. Su, F. Du, A. Wang, Y. Chen *et al.*, Sci. China Phys. Mech. Astron. **64**, 107462 (2021).

[28] C. Zhao, L. Wang, W. Xia, Q. Yin, J. Ni, Y. Huang, C. Tu, Z. Tao, Z. Tu, C. Gong *et al.*, arXiv:2102.08356 (2021).

[29] M. L. Kiesel, C. Platt, and R. Thomale, Phys. Rev. Lett. **110**, 126405 (2013).

[30] W.-S. Wang, Z.-Z. Li, Y.-Y. Xiang, and Q.-H. Wang, Phys. Rev. B **87**, 115135 (2013).

[31] X. Wu, T. Schwemmer, T. Müller, A. Consiglio, G. Sangiovanni, D. Di Sante, Y. Iqbal, W. Hanke, A. P. Schnyder, M. M. Denner *et al.*, Phys. Rev. Lett. **127**, 177001 (2021).

[32] C. Wen, X. Zhu, Z. Xiao, N. Hao, R. Mondaini, H. Guo, and S. Feng, Phys. Rev. B **105**, 075118 (2022).

[33] Y.-P. Lin and R. M. Nandkishore, Phys. Rev. B **106**, L060507 (2022).

[34] H. Chen, H. Yang, B. Hu, Z. Zhao, J. Yuan, Y. Xing, G. Qian, Z. Huang, G. Li, Y. Ye *et al.*, Nature (London) **599**, 222 (2021).

[35] S. Zhou and Z. Wang, Nat. Commun. **13**, 7288 (2022).

[36] Y. Xiang, Q. Li, Y. Li, W. Xie, H. Yang, Z. Wang, Y. Yao, and H.-H. Wen, Nat. Commun. **12**, 6727 (2021).

[37] L. Nie, K. Sun, W. Ma, D. Song, L. Zheng, Z. Liang, P. Wu, F. Yu, J. Li, M. Shan *et al.*, Nature (London) **604**, 59 (2022).

[38] F. Grandi, A. Consiglio, M. A. Sentef, R. Thomale, and D. M. Kennes, Phys. Rev. B **107**, 155131 (2023).

[39] M. Kang, S. Fang, J.-K. Kim, B. R. Ortiz, S. H. Ryu, J. Kim, J. Yoo, G. Sangiovanni, D. Di Sante, B.-G. Park *et al.*, Nat. Phys. **18**, 301 (2022).

[40] R. Lou, A. Fedorov, Q. Yin, A. Kuibarov, Z. Tu, C. Gong, E. F. Schwier, B. Büchner, H. Lei, and S. Borisenko, Phys. Rev. Lett. **128**, 036402 (2022).

[41] H. Luo, Q. Gao, H. Liu, Y. Gu, D. Wu, C. Yi, J. Jia, S. Wu, X. Luo, Y. Xu *et al.*, Nat. Commun. **13**, 273 (2022).

[42] S. Wu, B. R. Ortiz, H. Tan, S. D. Wilson, B. Yan, T. Birol, and G. Blumberg, Phys. Rev. B **105**, 155106 (2022).

[43] R. Tazai, Y. Yamakawa, S. Onari, and H. Kontani, Sci. Adv. **8**, eabl4108 (2022).

[44] X. Y. Feng, Z. Zhao, J. Luo, J. Yang, A. F. Fang, H. T. Yang, H. J. Gao, R. Zhou, and G.-q. Zheng, npj Quantum Mater. **8**, 23 (2023).

[45] J. Luo, Z. Zhao, Y. Zhou, J. Yang, A. Fang, H. Yang, H. Gao, R. Zhou, and G.-q. Zheng, npj Quantum Mater. **7**, 30 (2022).

[46] Y. Hu, X. Wu, B. R. Ortiz, X. Han, N. C. Plumb, S. D. Wilson, A. P. Schnyder, and M. Shi, Phys. Rev. B **106**, L241106 (2022).

[47] S. Cho, H. Ma, W. Xia, Y. Yang, Z. Liu, Z. Huang, Z. Jiang, X. Lu, J. Liu, Z. Liu *et al.*, Phys. Rev. Lett. **127**, 236401 (2021).

[48] H. Li, G. Fabbris, A. H. Said, Y. Pai, Q. Yin, C. Gong, Z. Tu, H. Lei, J. Sun, J.-G. Cheng *et al.*, Nat. Commun. **13**, 6348 (2022).

[49] T. Park, M. Ye, and L. Balents, Phys. Rev. B **104**, 035142 (2021).

[50] R. Nandkishore, L. S. Levitov, and A. V. Chubukov, Nat. Phys. **8**, 158 (2012).

[51] L. Van Hove, Phys. Rev. **89**, 1189 (1953).
[52] N. D. Mermin and H. Wagner, Phys. Rev. Lett. **17**, 1133 (1966).
[53] R. M. Fernandes, A. V. Chubukov, J. Knolle, I. Eremin, and J. Schmalian, Phys. Rev. B **85**, 024534 (2012).
[54] C. M. Varma, Phys. Rev. B **73**, 155113 (2006).
[55] P. A. Lee, Phys. Rev. X **4**, 031017 (2014).
[56] C. Pépin, D. Chakraborty, M. Grandadam, and S. Sarkar, Annu. Rev. Condens. Matter Phys. **11**, 301 (2020).
[57] S. Sarkar, M. Grandadam, and C. Pépin, Phys. Rev. Res. **3**, 013162 (2021).
[58] Y. Wang and A. Chubukov, Phys. Rev. B **90**, 035149 (2014).
[59] A. M. Tsvelik and A. V. Chubukov, Phys. Rev. B **89**, 184515 (2014).
[60] S. Sarkar, D. Chakraborty, and C. Pépin, Phys. Rev. B **100**, 214519 (2019).
[61] S.-W. Kim, H. Oh, E.-G. Moon, and Y. Kim, Nat. Commun. **14**, 591 (2023).
[62] Y. Song, T. Ying, X. Chen, X. Han, X. Wu, A. P. Schnyder, Y. Huang, J.-g. Guo, and X. Chen, Phys. Rev. Lett. **127**, 237001 (2021).
[63] B. Song, T. Ying, X. Kong, W. Xia, Q. Yin, C. Tu, C. Zhao, D. Dai, K. Meng, Z. Tao, Z. Tu *et al.*, Nat. Commun. **14**, 2492 (2023).
[64] T. Wang, A. Yu, H. Zhang, Y. Liu, W. Li, W. Peng, Z. Di, D. Jiang, and G. Mu, arXiv:2105.07732 (2021).
[65] N. Ratcliff, L. Hallett, B. R. Ortiz, S. D. Wilson, and J. W. Harter, Phys. Rev. Mater. **5**, L111801 (2021).
[66] J. Zhao, W. Wu, Y. Wang, and S. A. Yang, Phys. Rev. B **103**, L241117 (2021).
[67] Y. Hu, X. Wu, B. R. Ortiz, S. Ju, X. Han, J. Ma, N. C. Plumb, M. Radovic, R. Thomale, S. D. Wilson *et al.*, Nat. Commun. **13**, 2220 (2022).
[68] J. V. José, L. P. Kadanoff, S. Kirkpatrick, and D. R. Nelson, Phys. Rev. B **16**, 1217 (1977).
[69] I. L. Aleiner, D. E. Kharzeev, and A. M. Tsvelik, Phys. Rev. B **76**, 195415 (2007).
[70] M. M. Anber, E. Poppitz, and M. Ünsal, J. High Energy Phys. 04 (2012) 040.
[71] M. M. Anber, S. Collier, and E. Poppitz, J. High Energy Phys. 01 (2013) 126.
[72] P. Lecheminant, Phys. Lett. B **648**, 323 (2007).
[73] F.-Y. Wu, Rev. Mod. Phys. **54**, 235 (1982).
[74] P. Di Francesco, P. Mathieu, and D. Sénéchal, *Conformal Field Theory* (Springer-Verlag, New York, 1997).
[75] A. M. Tsvelik and A. B. Kuklov, New J. Phys. **14**, 115033 (2012).
[76] Y. He, Y. Yin, M. Zech, A. Soumyanarayanan, M. M. Yee, T. Williams, M. C. Boyer, K. Chatterjee, W. D. Wise, I. Zeljkovic *et al.*, Science **344**, 608 (2014).
[77] D. F. Agterberg and H. Tsunetsugu, Nat. Phys. **4**, 639 (2008).
[78] E. Berg, E. Fradkin, and S. A. Kivelson, Nat. Phys. **5**, 830 (2009).
[79] L. Radzihovsky and A. Vishwanath, Phys. Rev. Lett. **103**, 010404 (2009).
[80] E. Babaev, Nucl. Phys. B **686**, 397 (2004).
[81] J. Ge, P. Wang, Y. Xing, Q. Yin, H. Lei, Z. Wang, and J. Wang, arXiv:2201.10352 (2022).